smart cities

MDPI

Article

Solutions for Retrofitting Catenary-Powered Transportation Systems Toward Greater Electrification in Smart Cities

Rudolf Francesco Paternost, Riccardo Mandrioli, Vincenzo Cirimele, Mattia Ricco * and Gabriele Grandi

Department of Electrical, Electronic, and Information Engineering, University of Bologna, 40136 Bologna, Italy; rudolf.paternost@unibo.it (R.F.P.); r.mandrioli@unibo.it (R.M.); vincenzo.cirimele@unibo.it (V.C.); gabriele.grandi@unibo.it (G.G.)

* Correspondence: mattia.ricco@unibo.it; Tel.: +39-05120-93591

Highlights:

What are the main findings?

- Catenary-powered transport systems do not need substantial infrastructure updates to support a huge increase in load demand that can reach up to 4 times the current daily energy demand.
- A neutral impact on the overall operational efficiency of the catenary system can be achieved if the round-trip efficiency of the converter–battery block is at least 90.0%. Some scenarios with bigger battery pack capacity require 94.4% of round-trip efficiency.

What is the implication of the main finding?

- **Scalability of catenary-powered systems**: The work demonstrates that trolleybus networks (case study) are a scalable, robust, future-proof option for cities looking to electrify or expand their public transportation without incurring significant costs related to infrastructure reinforcement.
- **Efficiency requirements for battery systems integration**: Achieving the mentioned levels of round-trip efficiency for the converter–battery block might become more challenging, potentially requiring more stringent system monitoring and optimization.

Abstract: Catenary-powered networks are expected to play a pivotal role in urban energy transition, due to the larger deployment of electric public transport, in-motion-charging (IMC) vehicles, and catenary-backed electric vehicle chargers. However, there are technical challenges that must be overcome to ensure the successful utilization of existing networks without compromising vehicle performance or compliance with network standards. This paper aims to validate the use of battery energy storage systems (BESS) built from second-life batteries as a means of retrofitting catenary-powered traction networks. The objective is to increase the network robustness without creating a negative impact on its overall operational efficiency. Consequently, more electrification projects can be implemented using the same network infrastructure without substantial modifications. Furthermore, a power management scheme is presented which allows the voltage and current range allowed in the catenary network and the BESS maximum charging rate to be controlled from user-defined values. The proposed control scheme is adept at customizing the BESS size for the specific application under consideration. Validation is performed on a case study of the trolleybus system in Bologna, Italy.

Keywords: catenary systems; in-motion-charging; energy storage systems; second-life batteries; energy savings

Citation: Paternost, R.F.; Mandrioli, R.; Cirimele, V.; Ricco, M.; Grandi, G. Solutions for Retrofitting Catenary-Powered Transportation Systems Toward Greater Electrification in Smart Cities. *Smart Cities* **2024**, *7*, 3853–3870. https://doi.org/10.3390/smartcities7060148

Academic Editor: Isam Shahrour

Received: 13 September 2024
Revised: 12 November 2024
Accepted: 5 December 2024
Published: 7 December 2024

1. Introduction

Reducing reliance on fossil fuels has become a key objective for the European Union [1]. A central strategy in achieving this objective is the electrification of mobility, particularly within urban settings. In European cities, this goal is being pursued by supporting the implementation of catenary-powered mass transportation systems, which include trolleybus systems and rail-based transport systems (RTSs) such as tramways, subways, and railways.

However, as urban transportation systems increasingly embrace electrification, technical challenges emerge in the network infrastructure. They include issues such as high voltage drops in areas distant from substations and elevated transmission loss. These challenges become especially significant in a future context where urban transportation networks are expected to evolve into an infrastructure accommodating smart devices, such as electric vehicles (EVs) and renewable energy sources (RESs). The literature presents works involving the integration of EVs in trolleygrids [2–4], railways [5–7], and tramways [8]. The integration of renewable energy sources integration into catenaries is explored in [9–12].

Furthermore, the transformation of urban transport systems also paves the way for future vehicle fleets. In the realm of trolleybus systems, these fleets are anticipated to consist of a next-generation of trolleybuses known as in-motion-charging (IMC). In contrast to conventional trolleybuses, which require an overhead contact line (OCL) for their entire route, IMC trolleybuses are equipped with an on-board battery that enables operation also in sections where an OCL is not available [13–16]. The battery is instead recharged along sections where the vehicle is connected to the OCL by requesting additional power from the network. The increase in required power needed to supply both vehicle traction and battery charging introduces technical difficulties related to high voltage drops and network ohmic loss. Voltage levels falling below a certain limit can lead to a loss of power to the trolleybus. This may result in speed reduction, or in extreme cases, a complete stop if the voltage drops significantly.

Some works, such as [17–20], propose improving the stability of the network by acting on the OCL's supply points, i.e., the traction substations (TSs), replacing the classical adopted diode rectifiers with active converters. However, this solution requires considerable investment and does not fully solve the problem of voltage drops in the OCL sections far from the TSs. As demonstrated in [21–24], an attractive solution can be achieved through the utilization of battery-based stationary energy storage systems (BESSs) placed at specific points along the OCL. An essential consideration regarding the deployment of mid-line BESSs for voltage drop reduction lies in the equilibrium between the loss incurred by the battery pack and converter versus the savings resulting from diminished loss within the network. A considerable body of research has been conducted on the utilization of energy storage systems (ESSs) for the recovery of braking energy in transportation networks, with a particular focus on tramways [25–27] and railways systems [28,29], where the overall energy savings have been demonstrated. However, if the primary objective of ESS usage is to reduce voltage drop, there is a lack of the literature on the interplay evaluation between internal ESS loss and the network's ohmic loss reduction, which is crucial for understanding the overall efficacy and trade-offs of such applications.

This work aims to validate BESSs as a solution in the process of retrofitting catenary-powered transportation networks. The objective is to enhance the network's robustness, which would facilitate a significant expansion in the number of vehicles that can operate in the catenary system, as well as the integration of emerging devices and new bus fleets. As a case study, the trolleygrid of Bologna (Italy) was selected because it is set to undergo the electrification of bus fleets as IMC trolleybuses. The BESS units are created by reorganizing decommissioned battery packs from IMC vehicles, establishing an environmentally and economically virtuous circle. The batteries have reached the end of their useful life for traction applications but still possess a residual capacity of approximately 70–80% and can be used for non-power-intensive stationary applications [30,31].

The value of this research lies in the clarification of the association between loss reduction in the OCL of urban transportation networks due to an overall rise in the OCL voltage level and the BESS's loss during charge and discharge (C&D) processes. This is particularly relevant for the application where voltage drop reduction is the major objective of BESS usage in the OCL. This analysis aims to clarify the advantages and disadvantages in terms of energy impact, in the view of offering a clear understanding of the implications for transportation companies that are considering similar advances in their network infrastructure. Furthermore, we also propose a power management scheme

adapted for integrating BESSs into the midsection of OCLs. The control scheme facilitates a user-interface definition for the BESS maximum C&D rates and also maximum/minimum voltages and current levels allowed in the OCL, taking into account technical compliance. This is of particular significance in the context of the utilization of second-life batteries (SLBs) as BESSs, as they are unable to operate with the original C&D rates that are typical of new batteries [32,33].

The manuscript is structured as follows. Section 2 presents the simulation procedure employed to analyze DC catenary-powered transportation systems. Section 3 defines the voltage drop minimization problem, taking into account the technical constraints on the BESS and on the OCL infrastructure. The proposed power management scheme is also explained. Section 4 briefly presents the infrastructure of the trolleybus system in Bologna, Italy, which is the case study for this work. It also explains the hypothetical scenarios where conventional bus routes are electrified as IMC trolleybuses. Section 5 presents the results regarding the impact of second-life-based BESSs on the refereed trolleygrid together with general suggestions on their use. Finally, a conclusion of the work is presented in Section 6.

2. Simulation Procedure for Catenary-Powered System Analysis

The simulation of catenary-powered transportation systems takes into account three main elements:

- The OCL, which in the case of trolleybus systems consists of positive and negative conductors. For RTSs, the negative conductor is replaced by grounded rails that close the electrical circuit.
- The electrical power supply infrastructure, which includes the TSs and the supply feeders for connection to the OCLs.
- The load, represented by the moving vehicles connected to the OCL.

Alongside these main elements, technical developments consider the integration of additional devices. For illustration purposes, a trolleybus system, used as the case study, is depicted in Figure 1, where a BESS is connected to the OCL.

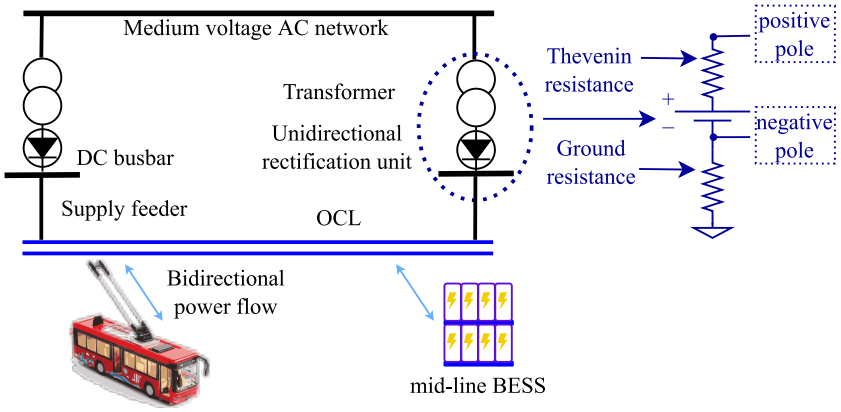

Figure 1. Electric schematic for powering DC trolleygrids considering the operation of a mid-line BESS.

The calculation of the catenary system state is performed using two simulation tools. The first one is a Simulink model that generates the vehicle's power absorption or injection (in the case of braking) over time. Further details on this process can be found in [34]. The second tool is a DC power flow algorithm that takes as input the information about the main elements already described and outputs the catenary voltage at each point and the current in every branch. In this algorithm, the network nodes can be divided into power nodes and voltage nodes. In the former ones, power is taken as input, and voltage is to be calculated; in the latter ones, voltage is taken as input, and power is to be calculated. All the electrical characteristics of the DC network are described by the nodal conductance matrix

G, which correlates voltages and currents at the network nodes. This matrix contains all the information necessary to describe the length and resistance of the wires that comprise the OCL, the supply feeders, the topology of the network, and the positions of the vehicles operating in the network, which vary over time. The current injection at a given node k can be presented as follows [35,36]:

$$I_k = V_k G_{kk} + \sum_{m \in \Omega_k} V_m G_{km}, \tag{1}$$

where V_k is the voltage of node k and Ω_k is the set of nodes m adjacent to node k having voltage V_m, with k varying from 1 up to the total number of nodes N. Each element of the conductance matrix is given as follows:

$$G_{km} = G_{mk} = -\frac{1}{r_{km}}, \quad G_{kk} = \sum_{m \in \Omega_k} \frac{1}{r_{km}}, \tag{2}$$

where r_{km} is the branch resistance between nodes k an m. In general, a conductance matrix is sparse because $G_{km} = 0$ whenever there is no connection between the two nodes. The power injection at a given node k can be represented by the following equation:

$$P_k = V_k^2 G_{kk} + V_k \sum_{m \in \Omega_k} V_m G_{km}. \tag{3}$$

The resulting non-linear system is solved through numerical methods, such as Newton–Raphson. The vehicles operating at the OCL are modeled as power nodes, where their power values are taken as the model's input and translated into voltages through an iterative process. TSs are modeled as voltage nodes in series with the compounded resistance of the transformer and rectification unit. Their voltage values are given by the substation nominal open-circuit voltage at the rectifier output (see Figure 1). Furthermore, ground resistance is also considered. The simulation algorithm performs a daily analysis with a time step of 1 s, thus enabling the acquisition of dynamic changes in the network as a series of 86,400 snapshots (i.e., solutions). The entire simulation procedure is in accordance with the flowchart presented in Figure 2 which is explained as follows.

Step 1: The algorithm starts by importing the data pertaining to the vehicles' positions and power, initializes a time counter, and creates the conductance matrices for the positive and negative poles, in the case of a trolleybus system. In RTSs, since the circuit is closed through the grounded rails, only the positive pole needs to be modeled. The trolleybuses' powers, for the case under study, were generated based on a Simulink model that emulates the behavior of conventional and IMC trolleybuses, described in [34].

Step 2: The iterative process solves the non-linear system (3). In a trolleybus network, the voltages at the positive and negative poles are calculated individually, and the vehicles' voltages are obtained by taking the difference between the potentials at the positive and negative poles. In an RTS, only the voltages at the positive pole need to be calculated.

Step 3: Convergence is achieved when the percentage difference between the vehicles' input power (P_{in}) and the power values calculated (P_{calc}) through the iterative process is lower than 0.1%.

Step 4: Decision step that verifies if the BESS actuates in the system or not.

Step 5: The BESS injects or absorbs a current based on the control trans-characteristics, as detailed in Section 3.

Step 6: A check on the time counter (represented by t in Figure 2) is performed to determine if the end of the day has been reached, at which point the simulation stops. If this has not been reached, the time counter and conductance matrices are updated to account for changes in the number, position, and power of the vehicles in operation.

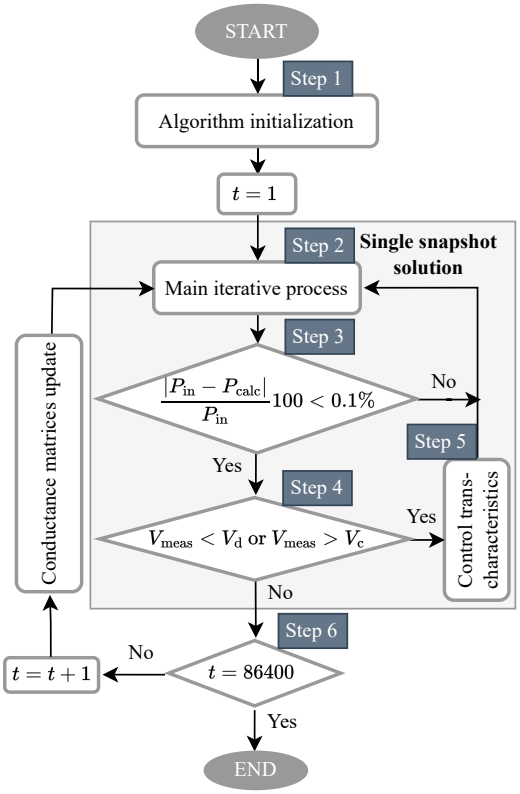

Figure 2. Flowchart of the catenary-powered traction system simulation procedure. P_{in} is the vehicles' input power, P_{calc} is the vehicles' power calculated by the iterative process, V_{meas} is the voltage measured at the BESS connection point, and V_c and V_d are the voltages for activating the BESS charging and discharging modes (see Section 3).

3. Voltage Drop Reduction in OCLs Considering Technical Constraints

3.1. Problem Formulation

It is assumed that the battery pack is connected to the OCL via a DC/DC converter as depicted in Figure 3. The BESS is designed to reduce the voltage drop in the middle of the OCL in an operation that controls the current injected by the BESS (I_H) depending on the voltage measurement at the output of the converter (V_H). Consequently, the voltage level reduction along the OCL, due to an expanded fleet with IMC buses (V_{IMC}) and the present conventional fleet (V_{conv}), can be minimized. Considering the limitations imposed by the battery C&D rate, voltage, and current limitations in the OCL, the minimization problem can be represented by (4), subject to the contracts (5):

$$\text{Minimize: } (V_{conv} - V_{IMC}), \tag{4}$$

$$\text{Subject to: } \begin{cases} V_{OCL}^{min} \leq V_H \leq V_{OCL}^{max} \\ I_H \leq I_{OCL}^{max} \\ I_{batt} \leq I_{batt}^{max} \end{cases}, \tag{5}$$

where V_{OCL}^{min} and V_{OCL}^{max} are the minimum and maximum voltages along the OCL; I_{OCL}^{max} is the maximum continuous current along the OCL; and I_{batt} is the battery pack current and I_{batt}^{max} is its maximum value, limited by the charging rate (C-rate).

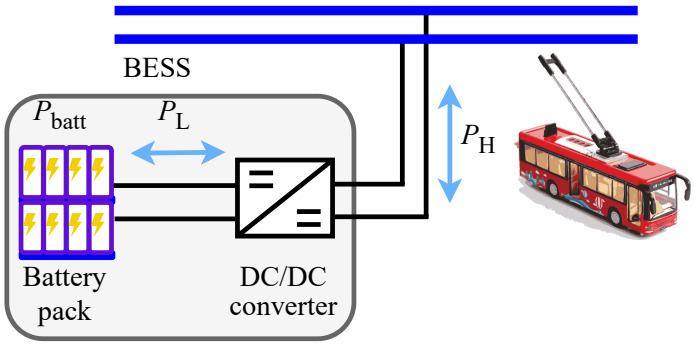

Figure 3. Schematic of a BESS connected to the OCL of a trolleygrid.

3.2. Proposed BESS Power Management Scheme

The BESS control operates under two conditions: the first is in accordance with the standard battery C&D processes, where the storage current varies linearly with OCL voltage; the second is in relation to the limited C&D, where the converter output current is constrained by the current on the battery side. Furthermore, the derived behaviour also considers the round-trip efficiency of the compounded block comprising batteries and the converter.

The power balance of the battery during C&D can be described by the following relations:

$$\text{charging} \rightarrow P_{batt} = \eta_{batt} P_L, \tag{6}$$

$$\text{discharging} \rightarrow P_{batt} = \frac{1}{\eta_{batt}} P_L, \tag{7}$$

where P_{batt} is the battery power, P_L is the power exchanged between the battery and the low voltage side of the converter, and η_{batt} is the battery efficiency. The power balance of the converter during C&D can be described by the following relationships:

$$\text{charging} \rightarrow P_L = \eta_{conv} P_H, \tag{8}$$

$$\text{discharging} \rightarrow P_L = \frac{1}{\eta_{conv}} P_H, \tag{9}$$

where P_H is the power exchanged between the converter high voltage side and the OCL (refer to Figure 3); η_{conv} is the converter efficiency. Hence, P_{batt} and P_H can be put in relation by means of the round-trip efficiency of the compounded block of battery and converter:

$$\text{charging} \rightarrow P_{batt} = \eta_{rt} P_H, \tag{10}$$

$$\text{discharging} \rightarrow P_{batt} = \frac{1}{\eta_{rt}} P_H, \tag{11}$$

where the round-trip efficiency of the block compounded by the battery and converter is defined as follows:

$$\eta_{rt} = \eta_{batt} \eta_{conv}. \tag{12}$$

Equations (10) and (11) can be rewritten in terms of voltage and currents as

$$\text{charging} \rightarrow V_{batt} I_{batt} = \eta_{rt} V_H I_H, \tag{13}$$

$$\text{discharging} \rightarrow V_{batt} I_{batt} = \frac{1}{\eta_{rt}} V_H I_H, \tag{14}$$

where V_{batt} is the battery voltage.

The C&D modes of the BESS are generally ruled by Equations (15) and (16) when no C-rate limitation is considered [23].

$$\text{charging} \rightarrow I_{\mathrm{H}} = s_{\mathrm{c}}(V_{\mathrm{H}} - V_{\mathrm{c}}), \tag{15}$$

$$\text{discharging} \rightarrow I_{\mathrm{H}} = s_{\mathrm{d}}(V_{\mathrm{H}} - V_{\mathrm{d}}), \tag{16}$$

where V_{d} is the voltage threshold measured at the connection point to the OCL that activates the BESS discharging mode. Conversely, the charging mode of the BESS is activated if the voltage level goes above the value V_{c}. Parameters s_{d} and s_{c} represent the discharging and charging slopes, respectively, and are calculated as follows:

$$\text{charging} \rightarrow s_{\mathrm{c}} = \frac{I_{\mathrm{H}}^{\max}}{V_{\mathrm{H}}^{\max} - V_{\mathrm{H}}}, \tag{17}$$

$$\text{discharging} \rightarrow s_{\mathrm{d}} = \frac{I_{\mathrm{H}}^{\max}}{V_{\mathrm{H}} - V_{\mathrm{H}}^{\min}}, \tag{18}$$

where $V_{\mathrm{H}}^{\max}$ and $V_{\mathrm{H}}^{\min}$ are the maximum and minimum voltages desired at the BESS connection point; $I_{\mathrm{H}}^{\max}$ is the maximum current at the converter's high voltage side.

Making reference to (13) and (14), the maximum converter output current $I_{\mathrm{H}}^{\max}$ for C&D takes the form:

$$\text{charging} \rightarrow I_{\mathrm{H}}^{\max} = \frac{1}{\eta_{\mathrm{rt}}} I_{\mathrm{batt}}^{\max} \frac{V_{\mathrm{batt}}}{V_{\mathrm{H}}}, \tag{19}$$

$$\text{discharging} \rightarrow I_{\mathrm{H}}^{\max} = -\eta_{\mathrm{rt}} I_{\mathrm{batt}}^{\max} \frac{V_{\mathrm{batt}}}{V_{\mathrm{H}}}. \tag{20}$$

For the charging process, the intersection between curves (15) and (19) leads to the borderline voltage value:

$$\text{charging} \rightarrow V_{\mathrm{H|bor}} = \frac{V_{\mathrm{c}}}{2} + \sqrt{\frac{V_{\mathrm{c}}^2}{4} + \frac{1}{\eta_{\mathrm{rt}}} \frac{I_{\mathrm{batt}}^{\max} V_{\mathrm{batt}}}{s_{\mathrm{c}}}}, \tag{21}$$

from where I_{H} starts to be ruled by (19) due to the C-rate limitation. For the discharging process, the intersection between (16) and (20) leads to the borderline voltage value:

$$\text{discharging} \rightarrow V_{\mathrm{H|bor}} = \frac{V_{\mathrm{d}}}{2} + \sqrt{\frac{V_{\mathrm{d}}^2}{4} - \eta_{\mathrm{rt}} \frac{I_{\mathrm{batt}}^{\max} V_{\mathrm{batt}}}{s_{\mathrm{d}}}}, \tag{22}$$

from which (20) starts to rule I_{H}.

To ensure that (22) results always in real values, the following inequality must be satisfied.

$$V_{\mathrm{d}}^2 - \eta_{\mathrm{rt}} \frac{4 I_{\mathrm{batt}}^{\max} V_{\mathrm{batt}}}{s_{\mathrm{d}}} \geq 0. \tag{23}$$

This means that current limitation during discharging occurs only if battery capacity C is lower than:

$$C = \frac{1}{\eta_{\mathrm{rt}}} \frac{s_{\mathrm{d}} V_{\mathrm{d}}^2}{4 I_{\mathrm{batt}}^{\max} V_{\mathrm{batt}}}. \tag{24}$$

The resulting possible values that I_{H} and I_{batt} can assume are described through the graph of Figure 4 together with the limitation imposed by the battery C-rate for different round-trip efficiencies. One can observe that, in the presented case, I_{batt} never exceeds the $I_{\mathrm{batt}}^{\max}$ value regardless of the compounded block efficiency.

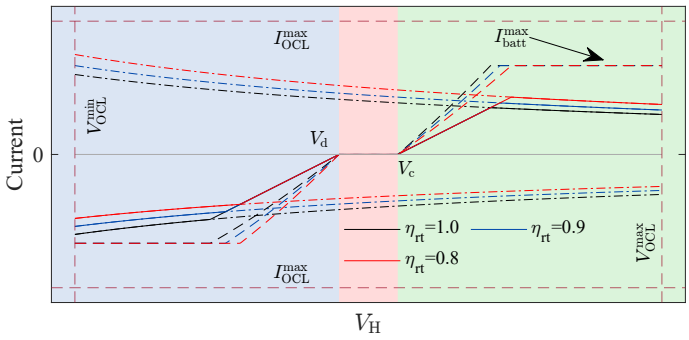

Figure 4. Control trans-characteristics considering different η_{rt} values. Solid lines represent I_H, dashed lines represent I_{batt}, dot-dashed lines indicate the current limitation imposed by battery C-rate. The blue area represents the discharge region, the green one represents the charging region, and the red area represents the idle region. Limitations on voltage and current of the OCL are represented by the wine-colored dashed lines.

3.3. Catenary-Powered Transportation System Efficiency Analysis

One of the key considerations in deploying the BESS in catenary systems relates to the additional loss that its operation can introduce in the system. The evaluation of this aspect entails an analysis of the daily energy E_{TSs} injected into the FS by the substations, the energy E_{veh} absorbed by the operating vehicles, the energy $E_{BESS|ch}$ absorbed by the BESS during the charging, and the energy $E_{BESS|ds}$ injected during discharging. The total network loss, L_{net}, can be defined as

$$L_{net} = E_{TSs} - (E_{veh} + L_{BESS}), \tag{25}$$

where the term L_{BESS} represents the BESS loss given by

$$L_{BESS} = E_{BESS|ch} - E_{BESS|ds} = E_{BESS|ch}(1 - \eta_{rt}^2). \tag{26}$$

The whole system loss can be then defined as

$$L_{sys} = L_{net} + L_{BESS}, \tag{27}$$

hence the overall system efficiency η_{sys} is defined as

$$\eta_{sys} = \frac{E_{veh}}{E_{TSs}} = \frac{E_{veh}}{E_{veh} + L_{net} + L_{BESS}}. \tag{28}$$

A minimum round-trip efficiency for each BESS size under examination can be determined to ensure that the BESS operation does not contribute to an increase in overall system loss. This condition is achieved if the BESS's loss is compensated by ohmic loss reduction in the OCL. This efficiency value is designated as the break-even efficiency ($\eta_{rt|bk}$) and is calculated on the condition that the network loss in the absence of the BESS operation $L_{net|NoBESS}$ is equal to the network loss with the BESS operation $L_{net|BESS}$ plus the BESS loss, i.e.:

$$L_{net|NoBESS} = L_{net|BESS} + L_{BESS}. \tag{29}$$

Defining ΔL as the difference between network loss without and with the BESS

$$\Delta L = L_{net|NoBESS} - L_{net|BESS}, \tag{30}$$

and making reference to (26), (29) becomes

$$\Delta L = E_{BESS|ch}(1 - \eta_{rt|bk}^2). \tag{31}$$

The BESS break-even efficiency can be expressed as

$$\eta_{\mathrm{rt|bk}} = \sqrt{1 - \frac{\Delta L}{E_{\mathrm{BESS|ch}}}}. \tag{32}$$

4. Case Study Definition

The electrical infrastructure of Bologna's trolleygrid consists of multiple feeding sections (FSs) supplied by TSs, which are typically situated at one or both ends. Figure 1 depicts an electrical schematic analogous to that of the FS named Marconi Trento-Trieste (FS MTT), which will serve as a reference in the study. In the FS MTT, the TS Marconi (TS M) supplies the system from the left side while the TS Trento-Trieste (TS TT) supplies from the right side.

A 12-pulse diode rectifier provides a DC voltage at the output of the TS with a rated value of 750 V. In accordance with the standard EN 50163 [37], the variation of the DC network's voltage level must remain within the 500–1000 V range at all points within the network. A TS is connected to the OCL through supply feeders and reinforcement feeders, as represented by dashed lines in Figure 5. The outward journey for the trolleybuses operating within the FS MTT commences in the vicinity of the TS M position, traversing the southern side of the FS and concluding in the vicinity of the TS TT, situated at a distance of 2200 m. The return journey of the trolleybuses covers a distance of 2500 m on the north side. The mid-line BESS was selected to be located at a distance of 900 m from the TS TT on a site outside the city's historic medieval walls, which presents no particular implementation constraints.

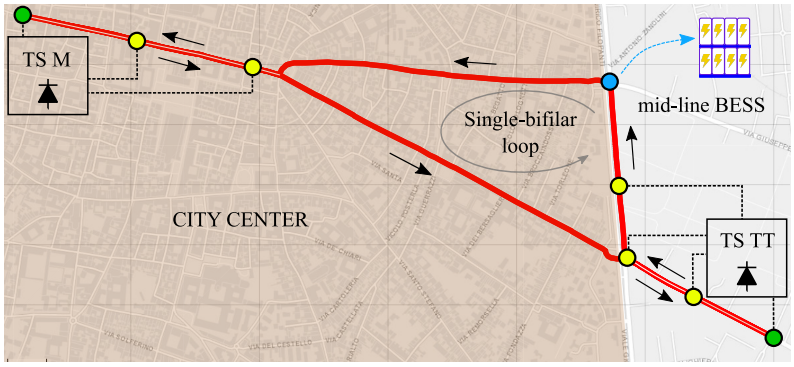

Figure 5. Topology of the FS MTT. Green circles indicate the position of supply feeders; yellow ones indicate the positions of reinforcement feeders and voltage stabilizers; the blue circle indicates the mid-line BESS position. The TS BESSs are positioned near the TS M and TS TT. Dashed lines represent the connection with the TSs. Arrows indicate the trolleybuses' travel directions.

4.1. Trolleybuses Operation in FS MTT

At present, two trolleybus lines are in operation within the FS MTT: line 14 and line 15. In addition, there are other lines within the same FS that are operated with buses equipped with diesel engines. One example is line 19, which has a considerable number of vehicles in operation.

In the upcoming plans for the development of electric urban mobility, lines 14 and 15 have been identified as potential candidates for the introduction of IMC trolleybuses. Similarly, line 19 will also undergo a switch to electric with vehicles equipped with IMC technology. Consequently, the scenario studied in this paper, referred to as the IMC scenario (IMC | S), considers lines 14, 15, and 19, all operated through IMC trolleybuses. Figure 6 depicts the number of vehicles running simultaneously in the analyzed FS during the day based on the timetables available at [38]. In the present scenario, only lines 14 and 15 utilize the OCL. On average, within an interval of 15 min, there are between 5 and 6 operating trolleybuses operating during the rush hours with a peak of 8 vehicles (Figure 6a). In

the future, when line 19 is also considered under the same FS, the maximum number of trolleybuses in circulation will simultaneously reach 11 with an average of 8 in the morning peak (Figure 6b).

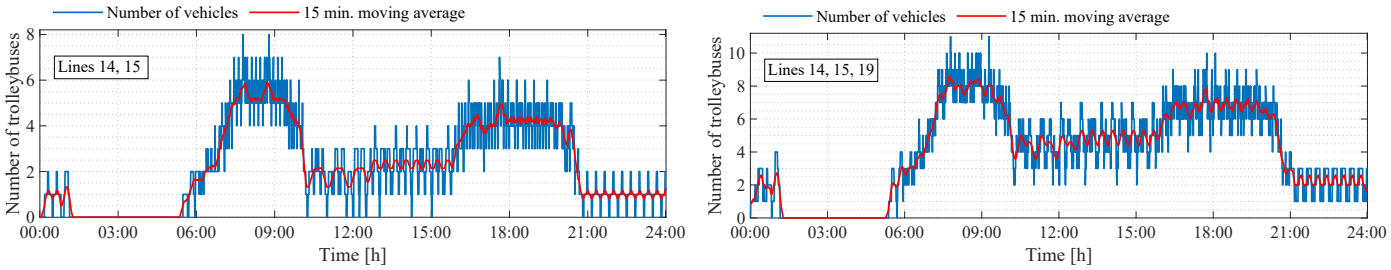

(**a**) (**b**)

Figure 6. Number of vehicles running in the FS MTT during the day. (**a**) Number of vehicles during operation of lines 14 and 15. (**b**): Number of vehicles during operation of lines 14, 15, and 19.

In order to gain a fair understanding of the evolution of power demand in IMC | S, this case is compared to the present condition which is then assumed to be a reference and indicated as the base-case scenario (BC | S). A comparison between BC | S and IMC | S scenarios in terms of currents at the output of TS M and TS TT over a one-day trolleybus system operation is shown in Figure 7. The current levels and their main time evolution for the BC | S were verified by means of a one-day measurement campaign carried out on TS TT [34] and is reported in the curve named base-case scenario measurements (BC | S Meas.) in Figure 7b. The reported voltage and current evolution results from averaging windows of 15 min. The comparison between the daily energy demand in the two scenarios is summarized in Table 1. The daily energy demanded increased by almost 300% for IMC | S. This notable increase is not solely attributable to the additional power required by IMC trolleybuses for charging the on-board battery. Rather, it is also a consequence of the fact that, in contrast to standard trolleybuses, the IMC types do not inject braking energy back into the network.

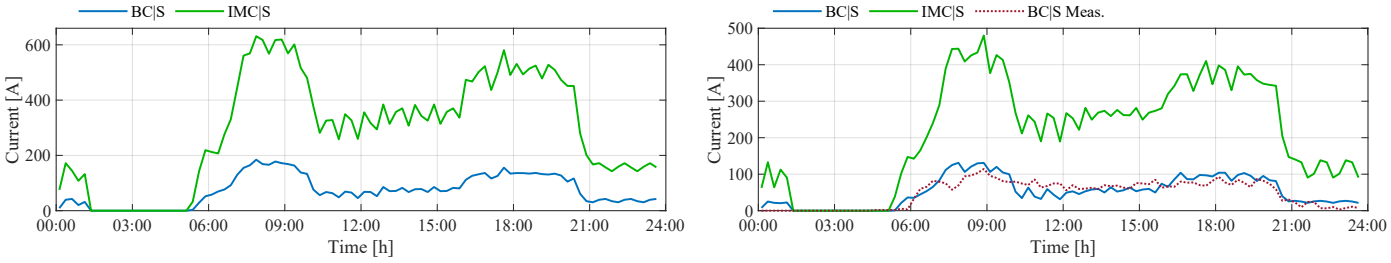

(**a**) (**b**)

Figure 7. Simulation results of currents in TS-M and TS-TT in an average window of 15 min. (**a**) Simulation results of current in TS-M. (**b**) Simulation results of current in TS-TT in comparison with current measurements.

Table 1. Daily energy for TS TT and TS M in the considered scenarios.

Traction Substation	Meas.	BC | S	IMC | S
Trento-Trieste	827 kWh	921 kWh	3774 kWh
Marconi	-	1283 kWh	5017 kWh
Total	-	2204 kWh	8791 kWh

As visible in Figure 8, the elevated demand for power in IMC | S resulted in unacceptable voltage drops along the OCL. It can be observed that the voltage levels reached 400 V in a section that extends for approximately 800 m, which violates the minimum voltage level of 500 V permitted for network operation. This condition can occur when more than

two trolleybuses operate consecutively in a critical area, making operation infeasible. The introduction of a mid-line BESS is specifically meant to circumvent this condition.

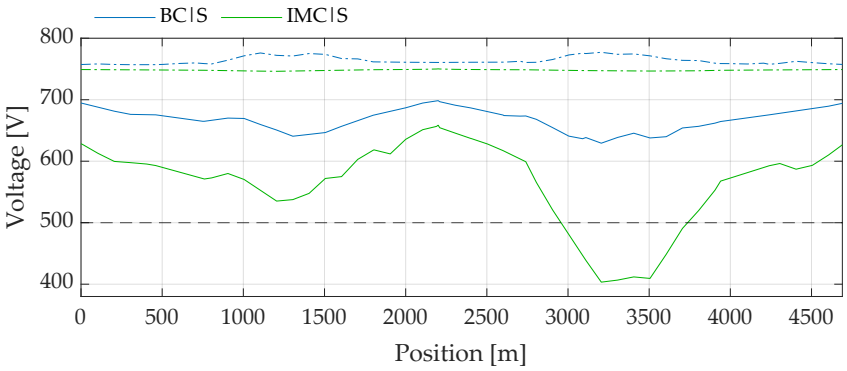

Figure 8. Voltage along the OCL for BC|S and IMC|S. Maximum (dot-dashed lines) and minimum values (solid lines). Black dashed line indicates the minimum allowed network voltage.

5. Analysis and Results

This section analyzes the results obtained by the simulation of the trolleygrid in the presence of the mid-line BESS under the operating conditions assumed for the scenario IMC|S detailed in Section 4.1. The analysis consists of evaluating voltage drop and current level reductions along the OCL for different BESS sizes. From these data, the operational efficiency of the trolleybus system with the C&D operations of the BESS is analyzed.

5.1. Considerations on Battery Pack and Control Technique

Based on the characteristics of Bologna's trolleygrid and the routes of different bus lines, IMC trolleybuses were designed to be equipped with battery packs with a nominal capacity of 60 kWh. In order to emulate the reuse condition of battery packs once they have reached the end of their useful life for traction applications, the BESS was constructed on the assumption that the useful capacity of the battery pack would be reduced according to a capacity loss of 20% due to the effects of aging and deterioration [31]. It was also assumed that one cycle of C&D would be carried out each day. Furthermore, the BESS was operated within a state of charge (SOC) range that always remained between 30% and 80% of its nominal capacity (C_{nom}), which ensured that the net BESS energy ($E_{\mathrm{BESS|net}}$) was always below the remaining capacity (C_{rem}), which is the battery energy after considering capacity loss. The daily simulation of the trolleybus system assumed that the BESS operated in discharging mode during periods of high power demand. This occurred in the morning between 06:00 and 11:00 and in the evening between 16:00 and 21:00 (see Figure 7). The charging process occurred between 00:00 and 06:00 when few vehicles operated within the network. Table 2 presents the results of the simulation, which shows the battery parameters considering the aforementioned characteristics of SLBs. It illustrates the number of single IMC trolleybus batteries that comprise the BESS, resulting in C_{nom} values of 120 kWh, 240 kWh, 360 kWh, and 480 kWh, as well as C_{rem}.

Table 2. Information on used IMC trolleybuses batteries to compose the BESS in function of idle region discharging voltage V_{d}.

V_{d}	IMC Batteries Count	C_{nom}	C_{rem}	$E_{\mathrm{BESS\|net}}$	SOC Range
650 V	2	120 kWh	96 kWh	54 kWh	35.0–80.0%
660 V	4	240 kWh	192 kWh	111 kWh	33.5–80.0%
670 V	6	360 kWh	288 kWh	165 kWh	34.0–80.0%
680 V	8	480 kWh	384 kWh	234 kWh	31.0–80.0%

The BESS actuation in the trolleygrid was carried out by fixing the maximum current $I_{\mathrm{H}}^{\mathrm{max}}$ injected into the network at 450 A, in accordance with the guidelines specified in EN

50119:2009, Annex A [39]. The minimum voltage at the BESS connection point, $V_{\mathrm{H}}^{\mathrm{min}}$, was set to 600 V. The values for the threshold voltage V_{d} were determined by analyzing the voltage at the BESS connection point for scenario IMC | S, taking into account the control parameters previously defined and the BESS capacities. These values were fixed at 650 V, 660 V, 670 V, and 680 V. As the value of V_{d} increased, the operational range of the BESS extended to larger voltage values, necessitating a larger BESS size.

In light of the reduced performance expected from the SLB-based BESS, the C&D operations were defined to never exceed a current equal to 1C. As demonstrated in [31], under such conditions an efficiency $\eta_{\mathrm{batt}} = 95\%$ could be assumed for the battery. The complexities involved in predicting SLB efficiency under higher C&D rates made this study exclusively consider a fixed maximum C-rate. It was assumed that the converter operated within a high-efficiency power range, and thus an approximate constant efficiency $\eta_{\mathrm{conv}} = 95\%$ was set. Consequently, a fixed round-trip efficiency $\eta_{\mathrm{rt}} = 90\%$ was assumed for the compounded block of the converter and battery (corresponding to the blue curve in Figure 4).

5.2. Beneficial Effects of Using Second-Life-Based BESS in Catenary Systems for Bus Fleet Electrification

The OCL voltage profile for scenario IMC | S is depicted in Figure 9, both without a BESS and with various nominal BESS capacities. It can be observed that the usage of BESS with a capacity of 120 kWh (i.e., 2 IMC batteries) did not provide significant improvements and did not even allow for maintaining the minimum voltage level above 500 V. This was due to the limitation imposed by the 1C discharging. It can be observed that as the number of batteries composing the BESS increased, there was a gradual increase in the OCL voltage level both in minimum voltage levels, 95% inter-percentile range, and average values. In the absence of a BESS, the voltage at the minimum voltage point (red arrow in Figure 9a) increased by 21%, 36%, 49%, and 61% for the respective considered capacities. As shown in Figure 10, the opposite trend was observed with the OCL's current, with the maximum value decreasing as the size of the BESS increased. A decrease in the current at the maximum point (red arrow in Figure 10a) by 26%, 45%, 62%, and 65% was achieved for the different considered capacities. The utilization of a capacity of 480 kWh (equivalent to 8 IMC trolleybus batteries) enabled the voltage profile to be maintained at a high level, with a minimum value that never fell below 550 V throughout the entire daily operation of the trolleybus system.

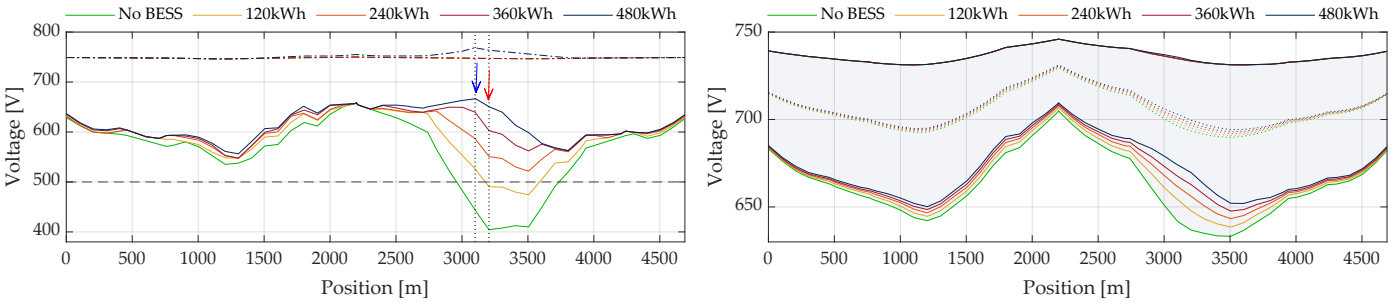

Figure 9. Voltage along the OCL considering the mid-line BESS operation in the network. TS-M is located at the extreme points on the right and left. TS-TT is around the middle position, at 2200 m. (**a**) Maximum (dot-dashed lines) and minimum voltage values (solid lines) along the OCL. Minimum allowed network voltage (black dashed line). The blue arrow indicates the mid-line BESS position. The red arrow indicates the minimum voltage point. (**b**) Average voltage values along the OCL (dotted lines) and 95% inter-percentile range (solid lines).

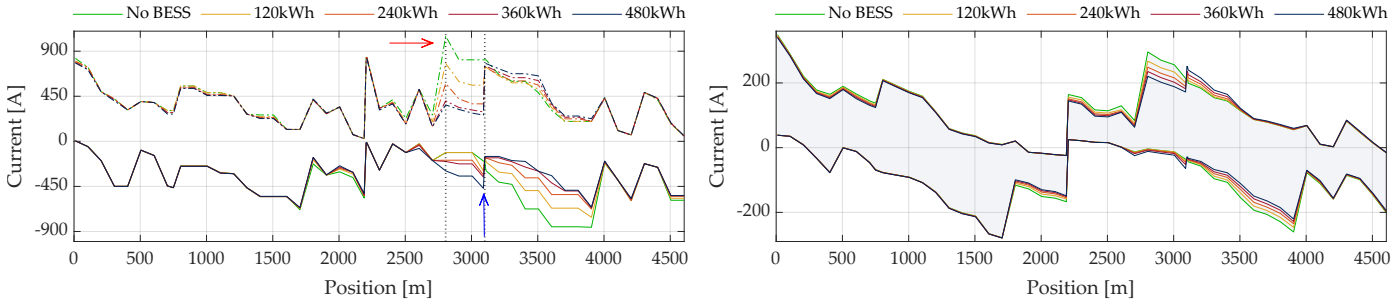

Figure 10. Current along the OCL considering the mid-line BESS operation in the network. TS-M is located at the extreme points on the right and left. TS-TT is located around the middle position, at 2200 m. (**a**) Maximum (dot-dashed lines) and minimum (solid lines) current values along the OCL. The red arrow indicates the maximum current point. The blue arrow indicates the mid-line BESS position. (**b**) The 95% inter-percentile range (solid lines) of current along the OCL.

The daily values of energies, losses, and efficiencies are presented in Table 3. It can be observed that there was a decrease in the OCL ohmic loss due to the overall increase in the OCL voltage level as the BESS capacity increased. However, the internal BESS loss increased due to the higher current handled by the device. This process resulted in a trade-off where the loss during the BESS C&D process exceeded the reductions in the OCL ohmic loss. This is evidenced by the increasing value of $\eta_{\mathrm{rt|bk}}$ required to maintain a neutral impact on the catenary-powered traction system's operation. In the worst-case scenario, employing a 480 kWh BESS necessitates $\eta_{\mathrm{rt|bk}} = 94.6\%$. It is worth noting that even in the cases where the system loss increased, the system efficiency remained practically unchanged, close to 95.5%. This result allows us to conclude that the use of the mid-line BESS made of SLBs has a quasi-neutral impact on the operating efficiency of the entire system, under the conditions specified in this work.

Table 3. Daily energy values used for the trolleybus system efficiency analysis.

V_{d}	E_{TSs}	E_{veh}	$E_{\mathrm{BESS\|ch}}$	$E_{\mathrm{BESS\|ds}}$	L_{net}	L_{BESS}	L_{sys}	η_{rt}	η_{sys}	$\eta_{\mathrm{rt\|bk}}$
-	8789 kWh	8406 kWh	-	-	383 kWh	-	383 kWh	-	95.6%	-
650 V	8789 kWh	8406 kWh	60 kWh	49 kWh	372 kWh	11 kWh	383 kWh	90.4%	95.6%	90.0%
660 V	8793 kWh	8406 kWh	123 kWh	100 kWh	364 kWh	23 kWh	387 kWh	90.2%	95.6%	91.8%
670 V	8800 kWh	8406 kWh	184 kWh	149 kWh	359 kWh	35 kWh	394 kWh	90.0%	95.5%	93.1%
680 V	8811 kWh	8406 kWh	260 kWh	211 kWh	356 kWh	49 kWh	405 kWh	90.1%	95.4%	94.6%

In a context where transportation companies can reuse their own decommissioned IMC batteries, the second-life-based BESS appears to be a promising option for enabling electrification projects without major infrastructure updates. However, it is crucial to maintain high BESS efficiency to ensure the catenary system operation without additional loss. SLBs may be the optimal choice for transportation companies without volume constraints in the local area of the device installation. In this case, it is necessary to include more decommissioned battery packs in the BESS to guarantee high efficiency of the device operation, rather than providing an increase in C&D rate levels. When space limitations are a major concern, opting for new batteries is a more advisable solution, as their nominal C-rate levels can be reached without significant efficiency decreases, which reduces the required battery capacity, thus minimizing the necessary space.

5.3. Comparison with Alternative Solutions for Reducing Voltage Drops

Alternative approaches are available for transportation companies to address voltage drops instead of solely relying on a BESS installed in mid-line positions. Some common alternatives include the following:

1. Reinforcement feeders (RFs) connecting vulnerable catenary positions to substations.
2. Implementing voltage regulation (VR) of substations by adjusting transformer taps.
3. Implementing dynamic regulation of substation voltage using controlled rectifiers.

Each solution has its own set of advantages and disadvantages. Reinforcement feeders connecting distant OCL positions, particularly through underground infrastructures that travel across the city center, may cause inconveniences if substations are distant from areas experiencing significant voltage drops. While increasing the voltage at the output of substations by adjusting transformer taps provides a relatively straightforward solution, it presents challenges in scenarios where both conventional and IMC trolleybuses operate. There is, indeed, a higher risk that the catenary voltage exceeds safety limits due to the braking energy injected by conventional trolleybuses. Moreover, the assumption that all IMC trolleybuses' braking energy is stored in on-board batteries may not always hold true, particularly if the batteries are already fully charged, potentially resulting in energy injection into the trolleygrid and violating voltage limits. Additionally, the actuation typically requires the system to be de-energized. Consequently, transportation companies using transformers capable of tap changers must set a fixed voltage level for the referenced TS, without the possibility of adjusting the transformer tap while the system is energized. Implementing dynamic voltage regulation via controlled rectifiers is costly and might not always yield effective results. Proper management of voltage drops along the line necessitates real-time monitoring and communication with substations for opportune rectifier action.

For the city of Bologna, the alternative solution of using additional RFs is illustrated in Figure 11, where a feeder (illustrated by a blue dashed line) connects the vulnerable OCL position (orange circle) to a stronger one. The effect in the network's voltage profile in comparison to the solutions using a mid-line BESS is exhibited in Figure 12. It is visible from the voltage profile that the inclusion of the RF was enough to keep the voltage under the limits of operation, for the studied case.

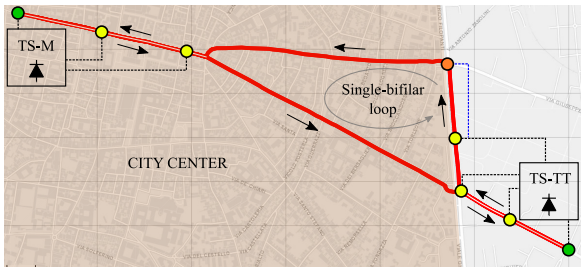

Figure 11. Topology of FS-MTT with an additional reinforcement feeder indicated by the blue dashed line. Green circles indicate the position of supply feeders and the extreme points of the FS; yellow ones indicate the positions of additional supply feeders and voltage stabilizers; the orange circle indicates the vulnerable OCL position. Arrows indicate the trolleybuses' travel directions.

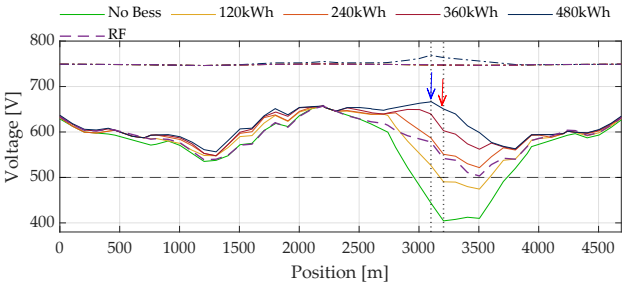

Figure 12. Maximum (dot-dashed lines) and minimum voltage values (solid lines) along the OCL in case of additional RF. Minimum voltages in the case of RF use are shown in the dashed violet line. The blue arrow indicates the reinforcement feeder position. The red arrow indicates the minimum voltage point.

To illustrate the impact of increasing the TS voltage level by changing the transformer's tap, two VR cases were presented, where the voltage values are defined based on the minimum required substation voltages needed to ensure that the catenary system maintains a minimum of 500 V throughout the entire day of operation. In the first case (VR Case 1), both substations had their rated voltages increased to 800 V (as shown in Figure 13). The increase in the voltage levels in TS-M is observable when comparing the extremes of the OCL, which are at a higher level (around 700 V), to the voltage level of the simulations considering BESS actuation (around 630 V). Similarly, the same voltage level increase in TS-TT is observable when comparing the curves at the position around 2200 m, where the refereed TS was nearby.

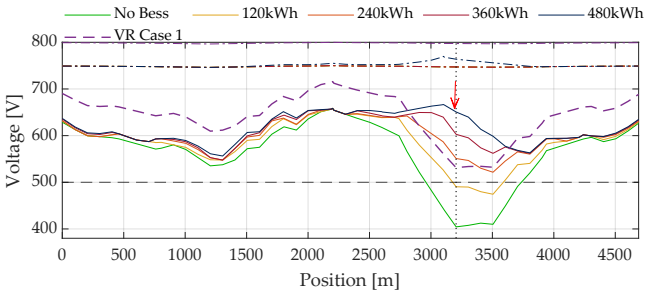

Figure 13. Maximum (dot-dashed lines) and minimum voltage values (solid lines) along the OCL in the case of the VRs in both TSs by changing transformer's tap. Minimum voltages in the case of the VRs are shown in the dashed violet line. The red arrow indicates the minimum voltage point.

In the second case (VR Case 2), only TS-TT had its rated voltage increased to 850 V, while TS-M remained at 750 V (Figure 14). This can be observed because only the OCL voltage near TS-TT position (2200 m) was increased (around 770 V), while the voltage level in the proximities of TS-M (extreme OCL positions) remained at the same levels in comparison with the simulations considering the BESS actuation. It is worth mentioning that this situation is feasible because TSs use diode rectification, which prevents reverse power flow between substations at different voltage levels.

A comparative analysis of voltage increase across various methods utilized for reducing voltage drop is presented in Table 4. It refers to the minimum voltage value acquired in the network during a daily operation. By observing the results, one can conclude that both the RF solution as well as the one involving transformer tap regulation can keep the voltage level above the minimum required threshold of 500 V. However, the greater voltage increase happened when BESSs of 360 kWh and 480 kWh were used, being able to raise the voltage by 35.6% and 37.6%, respectively. This increase was compared to the minimum voltage of 404 V when no methods for voltage increase were employed. Using a 240 kWh is comparable to employing tap-changing regulation in the transformer of both TSs (VR Case 1). The two solutions result in a 29.9% and 31.4% increase in voltage, respectively, compared with the minimum voltage of 404 V.

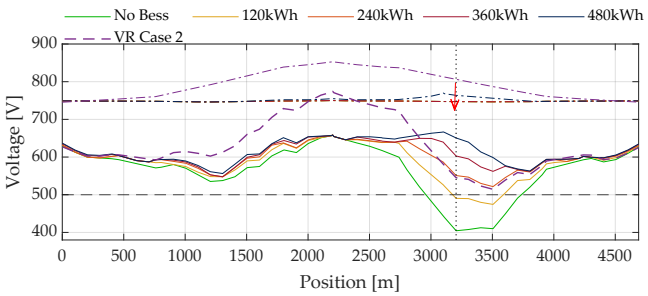

Figure 14. Maximum (dot-dashed lines) and minimum voltage values (solid lines) along the OCL in the case of VR only in the TS-TT by changing the transformer's tap. Minimum voltages in the case of VR are shown in the dashed violet line. The red arrow indicates the minimum voltage point.

Table 4. Quantitative comparison between the presented methods to reduce voltage drops.

	No BESS	120 kWh	240 kWh	360 kWh	480 kWh	RF	VR Case 1	VR Case 2
Minimum Voltage	404 V	474 V	522 V	548 V	556 V	503 V	531 V	514 V
Voltage Increase	-	17.3%	29.9%	35.6%	37.6%	24.5%	31.4%	27.2%

Although the solutions of including additional RFs and the increase of the voltage level using transformers with variable tap seems viable, the utilization of a mid-line BESS might be preferable for future catenary systems due to the following reasons:

- With the anticipated prevalence of IMC vehicles, repurposing SLBs from decommissioned ones can become a cost-effective option for transportation companies. The primary expenditure would be on the converter, rather than acquiring batteries, which would significantly reduce costs.
- Future catenary infrastructures are expected to incorporate PV systems. Mid-line BESSs can effectively capture surplus power generated by PV panels during periods when there are no nearby vehicles to absorb it. This approach mitigates energy losses that would be lost in PV curtailments by storing excess energy in mid-line BESS units.
- By strategically increasing the voltage level of the entire system beyond the minimum requirements (e.g., 500 V), overall voltage stability improves, thereby enhancing the operation of vehicles within the catenary network. This goal is more easily achievable through a power injection directly into the OCL by a storage solution due to the possibility of dynamic control.

6. Conclusions

This work evaluated the use of second-life-based battery energy storage systems as a solution in the process of retrofitting catenary-powered transportation systems. Taking a trolleybus system in the city of Bologna as a case study, it was assumed that the BESS would be constructed using batteries derived from the decommissioned battery packs of the same IMC trolleybuses that will be operational in the network. Therefore, particular considerations were made in terms of capacity loss, state of charge operating range, number of charging and discharging cycles, maximum discharging rate, and battery efficiency. The objective is to increase the overall voltage level and network's robustness, which would consequently allow a significant expansion in the number of vehicles to operate. This is especially valuable in a context where the power demand of future catenary systems tends to increase significantly due to the insertion of new devices, such as EV chargers and IMC trolleybuses. For the trolleybus system under study, the retrofitting solution allows the complete replacement of conventional trolleybuses currently operating in two bus lines and diesel buses in a third line with IMC trolleybuses.

The importance of this study consists of understanding how the reduction of losses in the OCL interacts with the losses in BESS operations due to the charge and discharge processes. In general, it is possible to conclude that the introduction of mid-line storage devices for purposes of voltage level increase in catenary networks can have a quasi-neutral impact on the overall catenary system efficiency operation in the case of a BESS composed of two decommissioned trolleybuses' on-board batteries, where the round-trip efficiency (battery and converter) required by the storage devices to guarantee a neutral efficiency impact is around 90.0%. Nevertheless, in a more aggressive scenario where eight SLBs are used, the necessary round-trip efficiency of the storage system required to guarantee a neutral efficiency impact is 94.6%, which could be difficult to reach using decommissioned devices. Other methods for mitigating voltage drops are indeed viable, including the installation of additional reinforcement feeders linking vulnerable catenary points to more robust ones, as well as the implementation of voltage regulation at substations through transformer tap regulation mechanisms. Nevertheless, in the context of future catenary environments, the utilization of a mid-line BESS emerges as the preferred option. This

preference proceeds from its capability to facilitate dynamic voltage and power control along the line and its potential for achieving greater reductions in voltage drop.

The analysis carried out in this work was conducted using a tailored power management scheme able to control the battery pack C-rate, and the maximum values of voltage and currents allowed at the OCL at a user-defined value. The control scheme was used to size the BESS for the application under consideration. Future works can focus on using battery depreciation models that incorporate environmental conditions and other factors to deeply understand their impact on the overall efficiency of the catenary system. Additionally, future research could compare the cost-effectiveness of using new versus second-life batteries in retrofitting initiatives.

Author Contributions: Conceptualization, R.F.P. and R.M.; methodology, R.F.P. and R.M.; software, R.F.P.; validation, R.F.P., R.M., V.C., M.R. and G.G.; formal analysis, R.M., V.C., M.R. and G.G.; investigation, R.F.P., R.M., V.C., M.R. and G.G.; resources, M.R. and G.G.; data curation, R.F.P. and R.M.; writing—original draft preparation, R.F.P., R.M. and V.C.; writing—review and editing, R.F.P., R.M., V.C, M.R. and G.G.; visualization, R.F.P. and R.M.; supervision, M.R. and G.G. All authors have read and agreed to the published version of the manuscript.

Funding: This research received no external funding.

Institutional Review Board Statement: Not applicable.

Data Availability Statement: Dataset available on request from the authors.

Conflicts of Interest: The authors declare no conflicts of interest.

References

1. European Commission and Directorate-General for Climate Action. *Going Climate-Neutral by 2050: A Strategic Long-Term Vision for a Prosperous, Modern, Competitive and Climate-Neutral EU Economy*; Publications Office of the European Union: Luxembourg, 2019. Available online: https://eur-lex.europa.eu/resource.html?uri=cellar:b828d165-1c22-11ea-8c1f-01aa75ed71a1.0002.02/DOC_1&format=PDF (accessed on 12 July 2024).
2. Weisbach, M.; Schneider, T.; Maune, D.; Fechtner, H.; Spaeth, U.; Wegener, R.; Soter, S.; Schmuelling, B. Intelligent Multi-Vehicle DC/DC Charging Station Powered by a Trolley Bus Catenary Grid. *Energies* **2021**, *14*, 8399. [CrossRef]
3. Van der Horst, K.; Diab, I.; Mouli, G.R.C.; Bauer, P. Methods for increasing the potential of integration of EV chargers into the DC catenary of electric transport grids: A trolleygrid case study. *eTransportation* **2023**, *18*, 100271. [CrossRef]
4. Bartłomiejczyk, M.; Jarzebowicz, L.; Hrbáč, R. Application of Traction Supply System for Charging Electric Cars. *Energies* **2022**, *15*, 1448. [CrossRef]
5. Brenna, M.; Longo, M.; Yaïci, W. Modelling and Simulation of Electric Vehicle Fast Charging Stations Driven by High Speed Railway Systems. *Energies* **2017**, *10*, 1268. [CrossRef]
6. Fernández-Rodríguez, A.; Fernández-Cardador, A.; Cucala, A.P.; Falvo, M.C. Energy Efficiency and Integration of Urban Electrical Transport Systems: EVs and Metro-Trains of Two Real European Lines. *Energies* **2019**, *12*, 366. [CrossRef]
7. Hajian, M.; Tricoli, P. A Mixed 1-phase and 3-phase Vehicle Charging System from AC Rail Traction Power Network. In Proceedings of the 2021 IEEE 15th International Conference on Compatibility, Power Electronics and Power Engineering, Florence, Italy, 14–16 July 2021; pp. 1–6. [CrossRef]
8. Zhang, T.; Zhao, R.; Ballantyne, E.E.; Stone, D. Increasing urban tram system efficiency, with battery storage and electric vehicle charging. *Transp. Res. D Transp. Environ.* **2020**, *80*, 102254. [CrossRef]
9. Diab, I.; Saffirio, A.; Chandra-Mouli, G.R.; Bauer, P. A simple method for sizing and estimating the performance of PV systems in trolleybus grids. *J. Clean. Prod.* **2023**, *384*, 135623. [CrossRef]
10. Diab, I.; Scheurwater, B.; Saffirio, A.; Chandra-Mouli, G.R.; Bauer, P. Placement and sizing of solar PV and Wind systems in trolleybus grids. *J. Clean. Prod.* **2022**, *352*, 131533. [CrossRef]
11. Bartłomiejczyk, M. Potential Application of Solar Energy Systems for Electrified Urban Transportation Systems. *Energies* **2018**, *11*, 954. [CrossRef]
12. Cano, A.; Arévalo, P.; Benavides, D.; Jurado, F. Sustainable tramway, techno-economic analysis and environmental effects in an urban public transport. A comparative study. *Sustain. Energy Grids Netw.* **2021**, *26*, 100462. [CrossRef]
13. Bergk, F.; Biemann, K.; Lambrecht, U.; Prof, D.; Pütz, R. Potential of In-Motion Charging Buses for the Electrification of Urban Bus Lines. *J. Earth Sci. Geotech. Eng.* **2016**, *6*, 347–362.
14. Wołek, M.; Szmelter-Jarosz, A.; Koniak, M.; Golejewska, A. Transformation of Trolleybus Transport in Poland. Does In-Motion Charging (Technology) Matter? *Sustainability* **2020**, *12*, 9744. [CrossRef]
15. Wołek, M.; Wolański, M.; Bartłomiejczyk, M.; Wyszomirski, O.; Grzelec, K.; Hebel, K. Ensuring sustainable development of urban public transport: A case study of the trolleybus system in Gdynia and Sopot (Poland). *J. Clean. Prod.* **2021**, *279*, 123807. [CrossRef]

16. Bartłomiejczyk, M. Practical application of in motion charging: Trolleybuses service on bus lines. In Proceedings of the 2017 18th International Scientific Conference on Electric Power Engineering (EPE), Kouty nad Desnou, Czech Republic, 17–19 May 2017; pp. 1–6. [CrossRef]
17. Zhang, D.; Jiang, J.; Wang, L.Y.; Zhang, W. Robust and Scalable Management of Power Networks in Dual-Source Trolleybus Systems: A Consensus Control Framework. *IEEE Trans. Intell. Transp. Syst.* **2016**, *17*, 1029–1038. [CrossRef]
18. Zhang, D.; Wang, L.Y.; Jiang, J.; Zhang, W. Load Prediction and Distributed Optimal Control of On-Board Battery Systems for Dual-Source Trolleybuses. *IEEE Trans. Transport. Electrific.* **2017**, *3*, 284–296. [CrossRef]
19. Zhang, D.; Wang, L.Y.; Jiang, J.; Zhang, W. Optimal Power Management in DC Microgrids With Applications to Dual-Source Trolleybus Systems. *IEEE Trans. Intell. Transp. Syst.* **2018**, *19*, 1188–1197. [CrossRef]
20. Sindi, E.; Wang, L.Y.; Polis, M.; Yin, G.; Ding, L. Distributed Optimal Power and Voltage Management in DC Microgrids: Applications to Dual-Source Trolleybus Systems. *IEEE Trans. Transport. Electrific.* **2018**, *4*, 778–788. [CrossRef]
21. Bartłomiejczyk, M.; Jarzebowicz, L.; Kohout, J. Compensation of Voltage Drops in Trolleybus Supply System Using Battery-Based Buffer Station. *Energies* **2022**, *15*, 1629. [CrossRef]
22. Bartłmiejczyk, M.; Jarzebowicz, L. Utility analysis and rating of energy storages in trolleybus power supply system. In Proceedings of the 2020 Zooming Innovation in Consumer Technologies Conference (ZINC), Novi Sad, Serbia, 26–27 May 2020; pp. 237–241. [CrossRef]
23. Paternost, R.F.P.; Mandrioli, R.; Ricco, M.; Barbone, R.; Bonora, G.; Cirimele, V.; Grandi, G. Energy Storage Management in Support of Trolleybus Traction Power Systems. In Proceedings of the 2022 International Symposium on Power Electronics, Electrical Drives, Automation and Motion (SPEEDAM), Sorrento, Italy, 22–24 June 2022; pp. 252–257. [CrossRef]
24. Paternost, R.F.P.; Mandrioli, R.; Barbone, R.; Cirimele, V.; Loncarski, J.; Ricco, M. Impact of a Stationary Energy Storage System in a DC Trolleybus Network. In Proceedings of the 2022 IEEE Transportation Electrification Conference & Expo (ITEC), Anaheim, CA, USA, 15–17 June 2022; pp. 1211–1216. [CrossRef]
25. Iannuzzi, D.; Ciccarelli, F.; Lauria, D. Stationary ultracapacitors storage device for improving energy saving and voltage profile of light transportation networks. *Transp. Res. Part C Emerg. Technol.* **2012**, *21*, 321–337. [CrossRef]
26. Ciccarelli, F.; Del Pizzo, A.; Iannuzzi, D. Improvement of Energy Efficiency in Light Railway Vehicles Based on Power Management Control of Wayside Lithium-Ion Capacitor Storage. *IEEE Trans. Power Electron.* **2014**, *29*, 275–286. [CrossRef]
27. Ciccarelli, F.; Iannuzzi, D.; Kondo, K.; Fratelli, L. Line-Voltage Control Based on Wayside Energy Storage Systems for Tramway Networks. *IEEE Trans. Power Electron.* **2016**, *31*, 884–899. [CrossRef]
28. De la Torre, S.; Sánchez-Racero, A.J.; Aguado, J.A.; Reyes, M.; Martínez, O. Optimal Sizing of Energy Storage for Regenerative Braking in Electric Railway Systems. *IEEE Trans. Power Syst.* **2015**, *30*, 1492–1500. [CrossRef]
29. Cipolletta, G.; Delle Femine, A.; Gallo, D.; Luiso, M.; Landi, C. Design of a Stationary Energy Recovery System in Rail Transport. *Energies* **2021**, *14*, 2560. [CrossRef]
30. Hu, X.; Deng, X.; Wang, F.; Deng, Z.; Lin, X.; Teodorescu, R.; Pecht, M.G. A Review of Second-Life Lithium-Ion Batteries for Stationary Energy Storage Applications. *Proc. IEEE* **2022**, *110*, 735–753. [CrossRef]
31. Abdel-Monem, M.; Hegazy, O.; Omar, N.; Trad, K.; Van den Bossche, P.; Van Mierlo, J. Lithium-ion batteries: Comprehensive technical analysis of second-life batteries for smart grid applications. In Proceedings of the 2017 19th European Conference on Power Electronics and Applications (EPE'17 ECCE Europe), Warsaw, Poland, 11–14 September 2017; pp. P.1–P.16. [CrossRef]
32. Shahjalal, M.; Roy, P.K.; Shams, T.; Fly, A.; Chowdhury, J.I.; Ahmed, M.R.; Liu, K. A review on second-life of Li-ion batteries: Prospects, challenges, and issues. *Energy* **2022**, *241*, 122881. [CrossRef]
33. Hossain, E.; Murtaugh, D.; Mody, J.; Faruque, H.M.R.; Haque Sunny, M.S.; Mohammad, N. A Comprehensive Review on Second-Life Batteries: Current State, Manufacturing Considerations, Applications, Impacts, Barriers & Potential Solutions, Business Strategies, and Policies. *IEEE Access* **2019**, *7*, 73215–73252. [CrossRef]
34. Paternost, R.F.; Mandrioli, R.; Barbone, R.; Ricco, M.; Cirimele, V.; Grandi, G. Catenary-Powered Electric Traction Network Modeling: A Data-Driven Analysis for Trolleybus System Simulation. *World Electr. Vehicle J.* **2022**, *13*, 169. [CrossRef]
35. Monticelli, A. *State Estimation in Electric Power Systems: A Generalized Approach*; Springer Science & Business Media: New York, NY, USA, 2012.
36. Salih, M.; Baumeister, D.; Wazifehdust, M.; Steinbusch, P.; Zdrallek, M.; Mour, S.; Deskovic, P.; Küll, T.; Troullier, C. Impact assessment of integrating novel battery-trolleybuses, pv units and ev charging stations in a dc trolleybus network. In Proceedings of the 2nd E-Mobility Power System Integration Symposium, Stockholm, Sweden, 15 October 2018; pp. 1–6.
37. *EN 50163:2004+A2:2020*; Railway Applications—Supply Voltages of Traction Systems. CENELEC: Brussels, Belgium, 2020.
38. Trasporto Passeggeri Emilia-Romagna (TPER). Tutte le Linee. Available online: https://www.tper.it/orari (accessed on 31 May 2023).
39. *EN 50119:2009+A1:2013*; Railway Applications—Fixed Installations—Electric Traction Overhead Contact Lines. CENELEC: Brussels, Belgium, 2013.